Electronic Supplementary Information

In situ insertion of copper to form D_{3h} symmetric $[Cu_3Mo_8O_{32}]^{10-}$ heteroanion for templated Ag_{55} Nanocluster

Jin-Ping Gao,[a] Zhikai Qi,[a] Fu-Qiang Zhang,[a] and Xian-Ming Zhang*[a,b]

[a]Key Laboratory of Magnetic Molecules and Magnetic Information Materials (Ministry of Education), Institute of Chemistry and Culture, School of Chemistry & Material Science, Shanxi Normal University, Taiyuan 030006, P. R. China.
E-mail: zhangxm@sxnu.edu.cn.
[b]Key Laboratory of Interface Science and Engineering in Advanced Material (Ministry of Education), College of Chemistry & Chemical Engineering, Taiyuan University of Technology, Taiyuan, 030024, P. R. China.

Content

1. Experimental section

1.1 Synthesis of $[(Cu_3(Mo_4O_{16})_2@Ag_{55}(CyhS)_{43}(CH_3O)(COOCF_3)]\cdot 3H_2O$ (1)

$(CyhSAg)_n$ was prepared by reacting equivalent amounts of $AgNO_3$ and CyhSH in the presence of Et_3N. The mixture of $(CyhSAg)_n$ (0.0011 g, 0.05 mmol) and $Cu(COOCF_3)_2$ (0.0060g, 0.025mmol) were dissolved in methanol and *N,N*-Dimethylformamide (7:1, 4 mL) under stirring. Half an hour later, copper powder (0.0030g, 0.025mmol) was added to the above solution. Finally, Na_2MoO_4 (0.001 g, 0.006 mmol) was the mixed solution after three hours. The reaction mixture was sealed and heated at 65°Cfor 20 hours (**Scheme S1**). Then, the solution crystallizes slowly when placed at room temperature after 5-7 days. Yellow-green octahedral block crystal of **1** was crystallized in the yields of 30%.

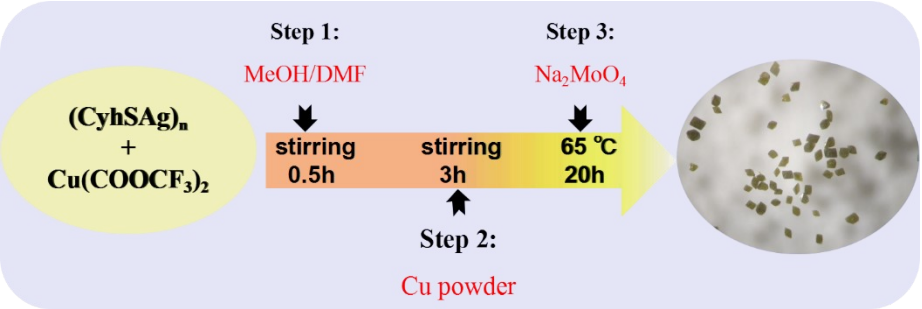

Scheme S1. Synthetic route to $Ag_{55}S_{43}$ clusters.

The suitable solvent system (CH_3OH/DMF) (DMF = dimethylformamide) and copper salt are very important. The central Cu atom in **1** is in a +2 oxidation state, which cannot be provided directly from common copper (II) salts such as $Cu(OAc)_2$, $(CF_3SO_3)_2Cu$, $CuCl_2$, or $Cu(NO_3)_2$ with Cu powder. Here, the copper powder has no effect on reducing the divalent copper, and the divalent copper is directly inserted into the intermediate connection position *in situ*.

1.2 Crystallographic studies. Single crystal of **1** with appropriate dimensions was chosen under an optical microscope and quickly coated with high vacuum grease (Dow Corning Corporation) to prevent decomposition. Crystal was mounted on CryoLoop™ loop and the cell parameter and intensity data were recorded on a Rigaku Oxford Diffraction XtaLAB Synergy-S diffractometer equipped with a HyPix-6000HE Hybrid Photon Counting (HPC) detector operating in shutterless mode and an Oxford Cryosystems Cryostream 800 Plus at 150 K using Cu Kα (λ = 1.54184 Å) for **1** from PhotonJet micro-focus X-ray Source. Data were processed using the CrystAlisPro software suite. Absorption corrections were applied

by using the program CrysAlisPro (multi-scan).[S1] Crystal structure was examined using the Addsym subroutine of PLATON to ensure that no additional symmetry could be applied to the models. The structure was solved with direct methods and refined using Full-matrix least-squares based on F^2 with program SHELXL-97 within OLEX2.[S2] Due to the disorder of cyclohexanethiol in the outshell of the cluster some atoms were refined isotropically. The heavy residue peaks are in immediate proximity to sliver atoms were split. Appropriate restraints or constraints orders were applied to the atoms in the cluster. Crystallographic data and structure refinements of **1** are summarized in Table S1, and the selected bond distances and angles are listed in Table S2.

1.3 Physical measurements. UV-Vis absorption spectra were recorded on TU-1950 UV-Vis spectrophotometer at room temperature. The corresponding optical band gap was evaluated as a function of the Kubelka-Munk equation: $\alpha/S = (1-R)^2/2R$. Fourier-transform infrared (FTIR) spectra were obtained on a FTIR spectrophotometer (Thermo Nicolet 360). The X-ray photoelectron spectrum (XPS) spectra were obtained by the Thermo scientific K-Alpha$^+$ XPS with a monochromatic Al Ka X-ray source (1486.6 eV) operating at 72W (12kV, 6mA). Binding energies were referred to the C 1s peak of adventitious carbon at 284.8 eV. EDS-Mapping was obtained by JSM-7500F. The photocurrent test was carried out on a CHI660E electrochemistry workstation. 5 mg samples of **1** and naphthol (5 wt. %, 10 μL) were dispersed in 80 μL ethanol, this system is mixed for half an hour under ultrasound. Then mixed solution was transferred by pipette tips dropped on the cleaned ITO glass. The coated film was obtained after evaporation under room temperature. The prepared ITO glass film was used as working electrode, a Pt sheet as the counter electrode, and an Ag/AgCl electrode as the reference electrode. 0.2 M Na_2SO_4 aqueous was used as the medium.

2. Supporting tables

Table S1. Crystal data and structure refinement for **1**.

Compound	**1**
Empirical formula	$C_{261}H_{476}Ag_{55}Cu_3F_3Mo_8O_{38}S_{43}$
Formula weight	12548.96
Temperature	150.00 (11)
Crystal system	triclinic
Space group	*P*-1
a (Å)	23.3674(3)
b (Å)	23.7497(4)
c (Å)	38.3998(5)
α (°)	73.3300(10)
β (°)	75.2360(10)
γ (°)	73.6330(10)
V (Å^3)	19233.6(5)
Z	2
ρ_{calc} (g cm^{-3})	2.162
μ (mm^{-1})	26.673
F (*000*)	12138.0
Size (mm)	0.15 × 0.08 × 0.07
Reflections	214510
Data / parameters	80132/2588
R_1[a], wR_2[b] [I>2σ(I)]	0.1023/0.2827
R_1[a], wR_2[b] (all data)	0.1428/0.3083
$\Delta\rho_{max}/\Delta\rho_{min}$(eÅ^{-3})	3.27/-3.98

[a]$R_1 = \sum||F_0|-|F_c||/\sum|F_0|$. [b]w$R_2 = [\sum w(F_0^2-F_c^2)^2/\sum w(F_0^2)^2]^{1/2}$

Table S2. Selected bond lengths [Å] and angles [°] for **1**.

1			
Ag1-S1	2.683(6)	Ag34-S31	2.519(5)
Ag1-S3	2.472(7)	Ag34-O20	2.323(9)
Ag1-S4	2.644(6)	Ag35-Ag34	3.024(2)
Ag1-O38[1]	2.524(19)	Ag35-S20	2.755(7)
Ag2-S1	2.707(7)	Ag35-S21	2.460(5)
Ag2-S4	2.658(6)	Ag35-S30	2.501(5)
Ag2-S5	2.505(7)	Ag35-O17	2.560(10)
Ag3-Ag5	3.330(2)	Ag36-Ag35	3.022(2)
Ag3-Ag13	3.251(2)	Ag36-Ag21	3.298(2)
Ag3-Ag4	3.140(3)	Ag36-S21	2.517(6)
Ag3-Ag2	3.085(2)	Ag36-S22	2.787(5)
Ag3-S1	2.409(6)	Ag36-S31	2.514(5)
Ag3-S6	2.415(6)	Ag36-O18	2.416(9)
Ag4-Ag1	3.070(3)	Ag37-S31	2.417(6)
Ag4-Ag8	3.239(3)	Ag37-S32	2.418(6)
Ag4-Ag6	3.234(3)	Ag38-S32	2.489(5)
Ag4-S1	2.403(7)	Ag39-S23	2.444(4)
Ag4-S2	2.408(9)	Ag39-S33	2.431(4)
Ag5-Ag6	3.370(3)	Ag39-Ag38	3.151(7)
Ag5-S6	2.428(5)	Ag40-O26	2.510(10)
Ag5-S7	2.412(5)	Ag40-S34	2.435(4)
Ag6-S2	2.423(9)	Ag41-S33	2.455(4)
Ag6-S7	2.445(7)	Ag41-S34	2.621(5)
Ag6-O3	2.592(12)	Ag42-S34	2.478(4)
Ag7-Ag8	3.153(2)	Ag42-S35	2.443(5)
Ag7-Ag6	3.250(2)	Ag44-S27	2.508(5)
Ag7-S9	2.562(5)	Ag44-O27	2.342(9)
Ag7-S8	2.467(4)	Ag44-Ag45	3.245(3)
Ag7-O4	2.341(9)	Ag46-Ag34	3.374(2)
Ag7-Ag17	3.161(2)	Ag46-S38	2.511(7)
Ag8-S3	2.517(7)	Ag46-S30	2.783(6)
Ag8-S2	2.715(7)	Ag46-S37	2.416(6)
Ag8-S9	2.541(6)	Ag46-Ag33	3.366(8)
Ag8-O2	2.509(13)	Ag46-Ag45	3.227(4)
Ag9-Ag19	3.170(2)	Ag48-S32	2.610(5)
Ag9-Ag8	3.072(3)	Ag49-Ag46	3.122(3)
Ag9-S3	2.406(6)	Ag49-Ag47	3.289(3)
Ag9-S11	2.912(6)	Ag49-S38	2.383(7)
Ag9-S10	2.398(6)	Ag49-S41	2.382(6)
Ag10-Ag9	3.157(2)	Ag49-O31	2.576(11)
Ag10-Ag1	3.229(2)	Ag51-Ag52	2.961(4)
Ag10-S4	2.524(5)	Ag51-S35	2.371(6)
Ag10-S11	2.445(5)	Ag51-S43	2.395(8)
Ag10-O2	2.367(11)	Ag52-S42	2.322(15)
Ag11-Ag10	2.922(2)	Ag52-S43	2.344(12)
Ag11-S4	2.491(5)	Ag52-Ag5	3.131(3)
Ag11-S12	2.502(4)	Ag53-S41	2.546(7)
Ag11-O1	2.413(12)	Ag54-S39	2.397(7)
Ag12-Ag13	3.310(2)	Ag54-O30	2.457(12)
Ag12-S5	2.429(6)	Ag54-S40	2.418(6)
Ag12-S12	2.735(4)	Ag54-S40	2.408(9)

Ag12-S13	2.472(5)	Ag54-O30	2.490(14)
Ag12-Ag23	2.812(11)	Ag55-S20	2.355(10)
Ag13-S5	2.505(6)	Ag55-S19	2.347(8)
Ag13-S14	2.546(6)	Ag55-Ag32	3.320(5)
Ag13-S6	2.677(5)	Ag55-Ag20	3.083(3)
Ag13-O1	2.501(13)	Mo1-O2	1.737(11)
Ag13-Ag23	3.18(3)	Mo1-O3	1.745(11)
Ag14-Ag25	3.142(2)	Mo1O1	1.784(11)
Ag14-Ag13	3.223(2)	Mo1-O6	2.170(9)
Ag14-S14	2.502(6)	Mo1-O5	2.170(9)
Ag14-S15	2.440(4)	Mo1-O4	2.149(9)
Ag14-O5	2.318(9)	Mo2-O6	2.101(10)
Ag14-Ag24	2.912(16)	Mo2-O7	1.706(9)
Ag15-S15	2.361(4)	Mo2-O15	1.819(10)
Ag15-S16	2.389(6)	Mo2-O12	2.241(9)
Ag16-Ag15	2.845(2)	Mo2-O10	1.813(10)
Ag16-S7	2.749(5)	Mo2-O4	2.104(9)
Ag16-S16	2.398(6)	Mo3-O5	2.106(9)
Ag16-S8	2.462(5)	Mo3-O12	2.271(9)
Ag17-S8	2.466(5)	Mo3-O11	1.812(11)
Ag17-S17	2.634(5)	Mo3-O8	1.709(10)
Ag18-Ag7	2.940(2)	Mo3-O9	1.803(9)
Ag18-S9	2.478(5)	Mo3-O4	2.118(9)
Ag18-S18	2.448(5)	Mo4-O6	2.064(11)
Ag18-O10	2.487(10)	Mo4-O5	2.099(9)
Ag18-Ag17	2.971(2)	Mo4-O12	2.213(8)
Ag18-Ag31	3.208(5)	Mo4-O14	1.816(9)
Ag19-Ag55	3.140(3)	Mo4-O13	1.795(10)
Ag19-S10	2.421(6)	Mo4-O16	1.732(10)
Ag19-S9	2.639(6)	Mo5-O24	1.819(10)
Ag19-S19	2.658(6)	Mo5-O17	1.788(9)
Ag20-S11	2.306(6)	Mo5-O23	2.288(9)
Ag21-S12	2.509(4)	Mo5-O27	2.101(9)
Ag21-S22	2.477(5)	Mo5-O29	1.712(9)
Ag21-O14	2.474(9)	Mo5-O20	2.071(10)
Ag21-Ag22	3.004(4)	Mo6-O25	1.822(10)
Ag22-S13	2.460(5)	Mo6-O26	1.799(10)
Ag23-S13	2.565(14)	Mo6-O23	2.228(8)
Ag23-S14	2.224(19)	Mo6-O28	1.705(10)
Ag24-S14	2.390(8)	Mo6-O27	2.122(9)
Ag25-Ag15	3.275(3)	Mo6-O21	2.080(9)
Ag25-S24	2.532(6)	Mo7-O18	1.818(9)
Ag25-S25	2.692(5)	Mo7-O22	1.806(10)
Ag25-O11	2.462(10)	Mo7-O23	2.226(9)
Ag25-Ag24	3.307(15)	Mo7-O20	2.123(9)
Ag25-Ag26	2.856(13)	Mo7-O19	1.708(10)
Ag26-S34	2.762(13)	Mo7-O21	2.091(8)
Ag26-O26	2.556(16)	Mo8-O27	2.134(10)
Ag27-Ag15	3.210(2)	Mo8-O20	2.190(8)
Ag27-S25	2.384(5)	Mo8-O21	2.218(9)
Ag27-S17	2.349(5)	Mo8-O31	1.766(11)
Ag27-Ag3A	2.876(15)	Mo8O30	1.761(12)
Ag27-Ag26	3.063(13)	Mo8-O32	1.760(11)
Ag28-Ag27	3.034(2)	Cu1-O15	1.947(10)

Ag28-S25	2.463(5)	Cu1-O14	1.919(9)
Ag28-S26	2.415(6)	Cu1-O17	1.935(9)
Ag28-S34	2.676(5)	Cu1-O18	1.933(10)
Ag28-Ag29	3.239(2)	Cu2-O13	1.946(9)
Ag28-Ag26	2.249(14)	Cu2-O11	1.944(10)
Ag29-S26	2.357(6)	Cu2-O22	1.941(10)
Ag29-S27	2.437(5)	Cu2-O26	1.959(10)
Ag30-S27	2.404(5)	Cu3-O9	1.936(10)
Ag31-S28	2.512(7)	Cu3-O25	1.923(10)
Ag31-S19	2.627(11)	Cu3-O24	1.929(11)
Ag32-S29	2.372(8)	Cu3-O10	1.938(10)
Ag32-S28	2.407(7)		
Ag33-S30	2.285(6)		
Ag34-S30	2.501(5)		

Table S3. Bond Valence Sum (BVS) calculations for compounds **1** of $[Cu_3Mo_8O_{32}]^{10-}$.

Bond		D	BVS	Bond		D	BVS	Bond		D	BVS
Mo1	O2	1.737	1.58445	Mo2	O6	2.101	0.59218	Mo3	O5	2.106	0.58420
Mo1	O3	1.745	1.54915	Mo2	O7	1.706	1.72377	Mo3	O12	2.272	0.37316
Mo1	O1	1.784	1.39429	Mo2	O15	1.817	1.27406	Mo3	O11	1.811	1.29504
Mo1	O6	2.170	0.49196	Mo2	O12	2.240	0.40637	Mo3	O8	1.708	1.71017
Mo1	O5	2.171	0.48958	Mo2	O10	1.815	1.28387	Mo3	O9	1.803	1.32546
Mo1	O4	2.149	0.52058	Mo2	O4	2.103	0.58899	Mo3	O4	2.117	0.56643
			6.03004				**5.86926**				**5.85448**
Mo4	O6	2.064	0.65294	Mo5	O24	1.819	1.26596	Mo6	O25	1.823	1.25541
Mo4	O5	2.100	0.59330	Mo5	O17	1.788	1.37760	Mo6	O26	1.800	1.33424
Mo4	O12	2.213	0.43687	Mo5	O23	2.288	0.35664	Mo6	O23	2.228	0.41971
Mo4	O14	1.815	1.28072	Mo5	O27	2.100	0.59361	Mo6	O28	1.707	1.71554
Mo4	O13	1.796	1.35046	Mo5	O29	1.711	1.69885	Mo6	O27	2.123	0.55761
Mo4	O16	1.732	1.60622	Mo5	O20	2..072	0.64054	Mo6	O21	2.081	0.62471
			5.92053				**5.93322**				**5.90726**
Mo7	O18	1.818	1.27005	Mo8	O27	2.133	0.54305				
Mo7	O22	1.805	1.31617	Mo8	O20	2.190	0.46547				
Mo7	O23	2.225	0.42345	Mo8	O21	2.218	0.43123				
Mo7	O20	2.122	0.55868	Mo8	O31	1.767	1.45879				
Mo7	O19	1.709	1.70832	Mo8	O30	1.760	1.48878				
Mo7	O21	2.090	0.60972	Mo8	O32	1.759	1.48996				
			5.88640				**5.87731**				
Cu1	O15	1.946	0.48557	Cu2	O13	1.946	0.48641	Cu3	O9	1.938	0.49703
Cu1	O14	1.919	0.52317	Cu2	O11	1.943	0.48936	Cu3	O25	1.925	0.51500
Cu1	O17	1.934	0.50144	Cu2	O22	1.940	0.49353	Cu3	O24	1.930	0.50759
Cu1	O18	1.934	0.50226	Cu2	O26	1.957	0.47112	Cu3	O10	1.938	0.49630
			2.00356				**1.94043**				**2.01539**

Table S4. The structures and coordination modes of molybdate anion templates in silver clusters in the literature and this work.

Slilver cluster	Molybdate anion templates	Number of Ag	negative charges	Ref.
$[Ag_{42}\{Ho(W_5O_{18})_2\}(t\text{-}BuC{\equiv}C)_{28}Cl_4]OH$	 **$[Ho(W_5O_{18})_2]^{9-}$**	42	9	S3
$[(EuW_{10}O_{36})_2@Ag_{72}(tBuC{\equiv}C)_{48}Cl_2{\cdot}4BF_4]$	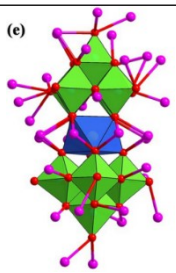 **$[EuW_{10}O_{36}]^{9-}$**	72	9	S4
$[Ag_{64}(C{\equiv}C^tBu)_{38}(CF_3COO)_8(Mn^{III}Mn^{IV}_2Mo_{14}O_{56})](OH){\cdot}10CH_3CN{\cdot}2H_2O$	 **$[Mn^{III}Mn^{IV}_2Mo_{14}O_{56}]^{17-}$**	42	17	S5
$[(Cu_3(Mo_4O_{16})_2@Ag_{55}(CyhS)_{43}(CH_3O)(COOCF_3)]{\cdot}3H_2O$	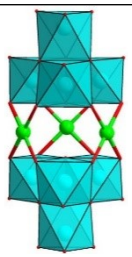 **$[Cu_3(Mo_4O_{16})]^{10-}$**	55	10	**This work**

3. Supporting figures

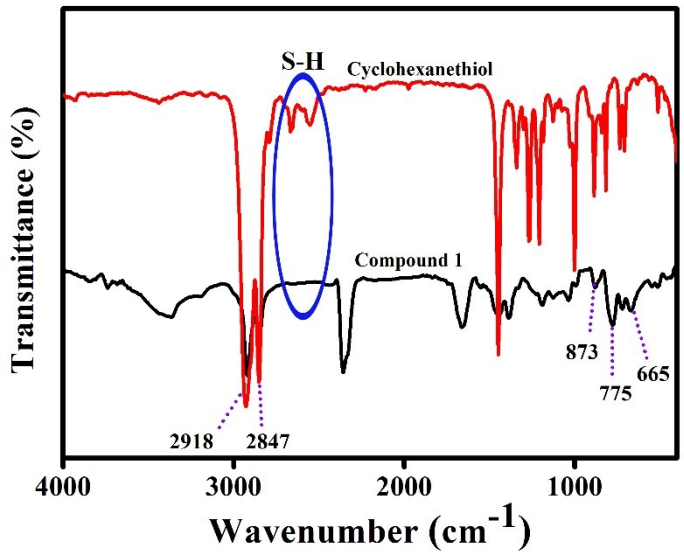

Fig. S1 FT-IR spectra of **1**.

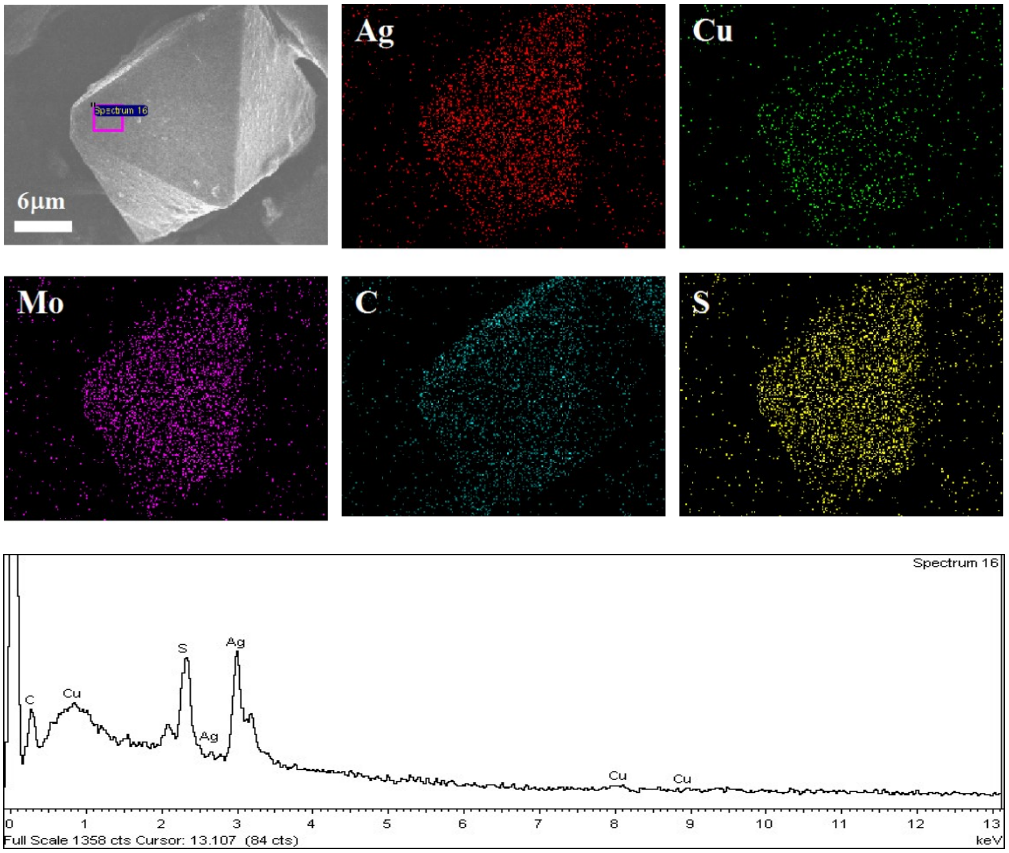

Fig. S2 Energy dispersive spectroscopy (EDS) mapping results on an SEM image of single particle of **1**. The scale bar is 6 µm.

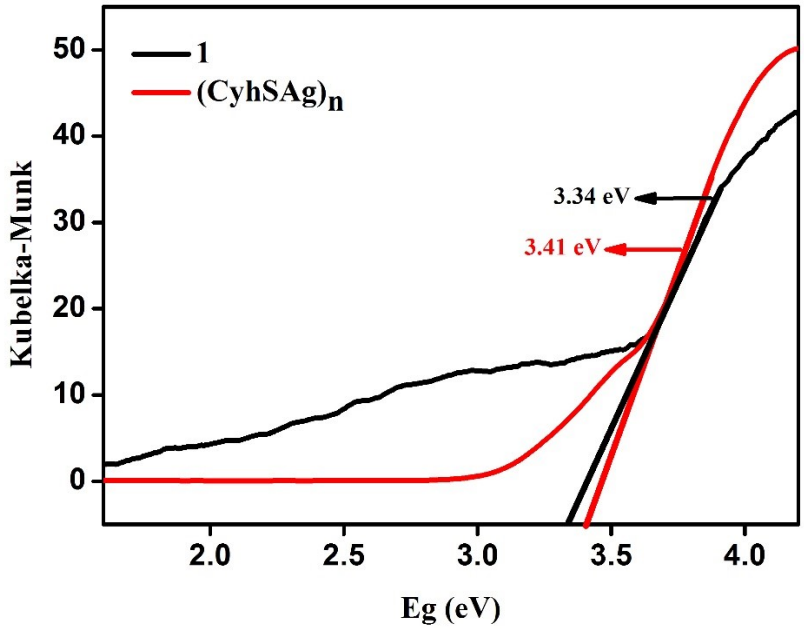

Fig S3. UV-vis diffuse spectra of **1**.

4. Supporting references

S1. (a) Rigaku Oxford Diffraction. CrysAlisPro Software system, version 1.171.40.68a, Rigaku Corporation: Oxford, UK, 2018; (b) Rigaku Oxford Diffraction. CrysAlisPro Software system, version 171.40.19a, Rigaku Corporation: Oxford, UK, 2018.

S2. Palatinus, L.; Chapuis, G. J. Appl. Crystallogr. 2007, 40, 786. Dolomanov, O. V.; Bourhis, L. J.; Gildea, R. J.; Howard, J. A. K.; Puschmann, H. J Appl. Crystallogr. 2009, 42, 339.

S3. Y.-Y. Li, F. Gao, J. E. Beves, Y.-Z. Li and J.-L. Zuo, *Chem. Commun.*, 2013, **49**, 3658-3660.

S4. S.-S. Zhang, H.-F. Su, Z. Wang, X.-P. Wang, W.-X. Chen, Q.-Q. Zhao, C.-H. Tung, D. Sun and L.-S. Zheng, *Chem. Eur. J.*, 2018, **24**, 1998-2003.

S5. J.-Y. Wang, K.-G. Liu, Z.-J. Guan, Z.-A. Nan, Y.-M. Lin and Q.-M. Wang, *Inorg. Chem*., 2016, **55**, 6833-6835.